

2009

Anisotropic magnetoresistance and planar Hall effect in epitaxial films of $\text{La}_{0.7}\text{Ca}_{0.3}\text{MnO}_3$

N. Naftalis

Y. Bason

J. Hoffman

X. Hong

C. H. Ahn

See next page for additional authors

Follow this and additional works at: <https://digitalcommons.unl.edu/physicshong>



Part of the [Atomic, Molecular and Optical Physics Commons](#), and the [Engineering Physics Commons](#)

Authors

N. Naftalis, Y. Bason, J. Hoffman, X. Hong, C. H. Ahn, and L. Klein

Anisotropic magnetoresistance and planar Hall effect in epitaxial films of $\text{La}_{0.7}\text{Ca}_{0.3}\text{MnO}_3$

N. Naftalis,^{1,a)} Y. Bason,¹ J. Hoffman,² X. Hong,² C. H. Ahn,² and L. Klein¹

¹*Department of Physics, Nano-magnetism Research Center, Institute of Nanotechnology and Advanced Materials, Bar-Ilan University, Ramat-Gan 52900, Israel*

²*Department of Applied Physics, Yale University, New Haven, 06520-8284 Connecticut, USA*

(Received 23 April 2009; accepted 18 June 2009; published online 22 July 2009)

We measured the anisotropic magnetoresistance (AMR) and the planar Hall effect (PHE) in a [001] oriented epitaxial thin film of $\text{La}_{0.7}\text{Ca}_{0.3}\text{MnO}_3$ (LCMO) as a function of magnetic field, temperature, and current direction relative to the crystal axes. We find that both AMR and PHE in LCMO depend strongly on the current orientation relative to the crystal axes, and we demonstrate the applicability of AMR and PHE equations based on a fourth order magnetoresistance tensor consistent with the film symmetry. © 2009 American Institute of Physics. [DOI: 10.1063/1.3176934]

I. INTRODUCTION

Doped manganites have been extensively studied since the observation of colossal magnetoresistance.¹ Special attention has been given to the magnetotransport properties of these materials, including their anisotropic magnetoresistance (AMR) and planar Hall effect (PHE).^{2,3} Recent studies of *c*-oriented $\text{La}_{0.8}\text{Sr}_{0.2}\text{MnO}_3$ (LSMO) thin films show that for a correct description of the AMR and the PHE in this compound, one needs to take into consideration the crystal-line contribution and expand the magnetoresistance tensor to fourth order using both the angle α between the magnetization (\mathbf{M}) and the [100] and the angle θ between the current (\mathbf{J}) and the [100] [see inset of Fig. 1(a)].⁴ Based on this expansion, the AMR, which describes the changes in the longitudinal resistivity (ρ_{long}), and the PHE, which describes the changes in the transverse resistivity (ρ_{trans}), are given as

$$\rho_{\text{long}} = A \cos(2\alpha - 2\theta) + B \cos(2\alpha + 2\theta) + C \cos(4\alpha) + D \quad (1)$$

and

$$\rho_{\text{trans}} = A \sin(2\alpha - 2\theta) - B \sin(2\alpha + 2\theta). \quad (2)$$

Here we study the AMR and the PHE in the manganite $\text{La}_{0.7}\text{Ca}_{0.3}\text{MnO}_3$ (LCMO). Previous studies of ρ_{long} and ρ_{trans} in this compound used the equations valid for amorphous and polycrystalline films, for which

$$\rho_{\text{long}} = \rho_{\perp} + (\rho_{\parallel} - \rho_{\perp}) \cos^2 \varphi, \quad (3)$$

$$\rho_{\text{trans}} = (\rho_{\parallel} - \rho_{\perp}) \sin \varphi \cos \varphi, \quad (4)$$

where ρ_{\parallel} and ρ_{\perp} are the resistivities parallel and perpendicular to the magnetization, respectively, and φ is the angle between \mathbf{J} and \mathbf{M} ; i.e., $\varphi = \alpha - \theta$. While deviations from Eqs. (3) and (4) were observed for LCMO,³ they were attributed to various extrinsic sources, and the applicability of the equations to LCMO was not questioned. Here we show that Eqs. (3) and (4) are not applicable, while Eqs. (1) and (2)

provide a good description of ρ_{long} and ρ_{trans} in LCMO. We note that when \mathbf{J} is along [100] or [010], Eq. (1) reduces to $\rho_{\text{long}} = C_0 + C_1 \cos^2 \alpha + C_2 \cos^4 \alpha$, a form used before to account for crystal contribution in various magnetic films including epitaxial films of Fe (Ref. 5) and Fe_3O_4 .⁶

II. SAMPLE CHARACTERIZATION

The thin films used for this study are [001] oriented epitaxial thin films of LCMO grown on single crystal SrTiO_3 (100) using off-axis magnetron sputtering. The growth temperature is 660 °C with process gases of 80% argon and 20% oxygen at a pressure of 150 mTorr.⁷ The deposition rate is ~ 1 nm/min and the sample is cooled in 1 atm O_2 . No additional postannealing is performed. X-ray diffraction measurements suggest that the film is partially relaxed, since its *c*-axis lattice constant (3.85 Å) is less than the bulk value (3.86 Å). X-ray reflectivity and θ -2 θ scans show that the film whose measurements are presented here is 32 nm in thick-

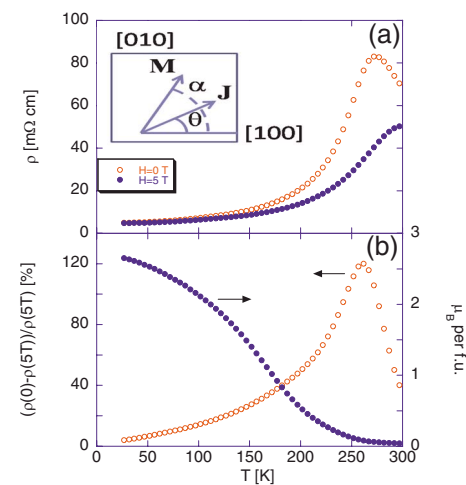


FIG. 1. (Color online) (a) Temperature dependence of the resistivity ρ in zero field (open symbols) and in a field of 5 T (close symbols). Inset: A sketch of the angles α and θ used in Eqs. (1) and (2). (b) Magnetization in units of $\mu_B/f.u.$ as a function of temperature while cooling in a field of 2000 Oe along [110], and magnetoresistance as a function of temperature in an in-plane field of 5 T.

^{a)}Electronic mail: naftaln@mail.biu.ac.il.

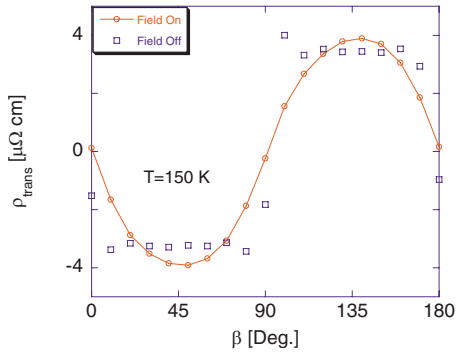


FIG. 2. (Color online) ρ_{trans} at $T=150$ K as a function of β , the angle between an in-plane applied field of 600 Oe and $[100]$. For each β ρ_{trans} is measured with field on and then with field off. The current direction is along $[100]$.

ness. The film was patterned by photolithography to allow ρ_{long} and ρ_{trans} measurements, with \mathbf{J} at different angles θ relative to $[100]$. Figure 1(a) presents the resistivity data of this film in zero field and in 5 T. The zero field resistivity peak temperature is ~ 275 K, close to the bulk value of this composition, and the effect of the applied field is typical. Figure 1(b) presents magnetization as a function of temperature while cooling in a field of 2000 Oe applied along $[110]$, and magnetoresistance in an in-plane field of 5 T. The films exhibit biaxial magnetocrystalline anisotropy with easy axes along $\langle 110 \rangle$ directions. This is demonstrated in Fig. 2, which shows that these are the directions of the remanent magnetization obtained after applying and removing a magnetic field in different directions. The biaxial anisotropy we find is consistent with Ref. 8 while in Ref. 9 the easy axes are along $\langle 100 \rangle$. The origin of this discrepancy is unclear.

III. RESULTS AND DISCUSSION

Figure 3 shows ρ_{long} and ρ_{trans} measurements at $T=125$ K. For convenience we subtract from ρ_{long} its average value, which is denoted as D in Eq. (1), and define it as $\Delta\rho_{\text{long}}$. The measurements were performed on patterns with different \mathbf{J} directions relative to $[100]$ (θ) as a function of the magnetization direction relative to $[100]$ (α). The measure-

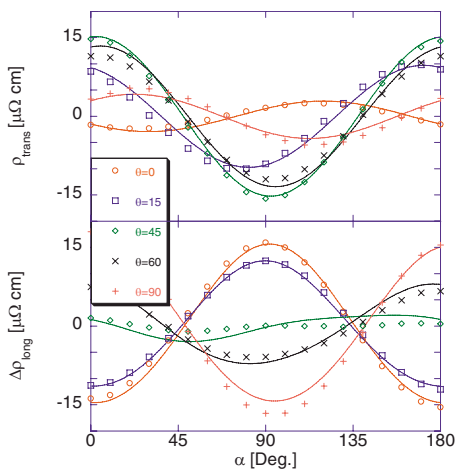


FIG. 3. (Color online) $\Delta\rho_{\text{long}}$ and ρ_{trans} of five patterns with different θ 's as a function of α at $T=125$ K. The solid lines are fits to Eqs. (1) and (2).

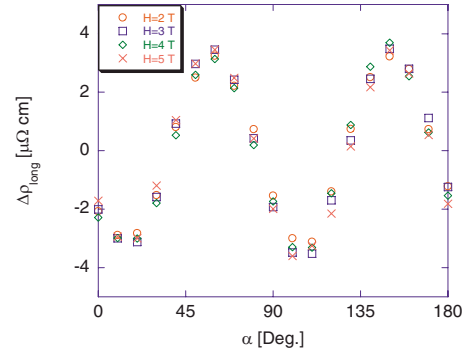


FIG. 4. (Color online) $\Delta\rho_{\text{long}}$ as a function of α for a pattern with $\theta=\pi/4$ with four different applied fields, at $T=25$ K.

ments were taken with a constant magnetic field of 4 T rotating in the plane of the film. The magnitude of the magnetic field we use is much larger than the anisotropy field; hence, the magnetization orientation is in the direction of the applied field. The deviation of the observed behavior from Eqs. (3) and (4), and the contribution of crystal symmetry are quite evident. Despite the fact that both $\Delta\rho_{\text{long}}$ and ρ_{trans} appear sinusoidal, the amplitudes of $\Delta\rho_{\text{long}}$ and ρ_{trans} for a given θ are different and they both depend on θ , inconsistent with Eqs. (3) and (4) according to which all amplitudes should be the same. Moreover, Fig. 4 shows that at $T=25$ K the crystal symmetry contribution becomes prominent and $\Delta\rho_{\text{long}}$ exhibits contributions with fourfold symmetry. Figure 4 also shows that exactly the same behavior is observed for different fields between 2 and 5 T indicating that the magnetization follows the applied field. This indicates that the fourfold symmetry is an intrinsic property of the resistivity tensor (as allowed by symmetry) and not a result of the effect of magnetocrystalline anisotropy on magnetic orientation. We note that fourfold symmetry in the AMR data was observed in other systems such as $(\text{Ga,Mn})\text{As}$.¹⁰

In view of the failure of Eqs. (3) and (4), we try to fit the data at $T=125$ K, for which we have AMR and PHE for five different θ 's, with Eqs. (1) and (2). We find that the *same* four fitting parameters $A=-8.79$, $B=-6.41$, $C=0.53$, and $D=6241$ (which is a constant shift) provide a good fit to all ten different AMR and PHE curves. This indicates that Eqs. (1) and (2), which were used successfully to fit the AMR and the PHE data of LSMO,⁴ provide a good description of the AMR and the PHE data for LCMO, as well.

The reported θ dependence of the amplitude is important for applications. Designing sensing devices¹¹ or memory devices¹² with manganites can benefit from increasing the signal by having the current in particular directions for which the AMR or the PHE signals attain their maximum values. As we can see, ρ_{trans} obtains its largest amplitude for $\theta = \pm \pi/4$ while the PHE and the AMR are often measured with $\theta=0, \pi/2$. The fact that the AMR and the PHE in LSMO and LCMO are described by Eqs. (1) and (2) and not by Eqs. (3) and (4), as previously assumed, suggests the need for a more extensive study of the magnetotransport properties of other manganites and other magnetic epitaxial films.

ACKNOWLEDGMENTS

L.K. acknowledges support by the Israel Science Foundation founded by the Israel Academy of Sciences and Humanities (Grant No. 577/07). The work at Yale is supported by NSF MRSEC Grant Nos. DMR 0520495 and DMR 0705799, NRI, ONR, and the Packard Foundation.

- ¹M. McCormack, S. Jin, T. H. Tiefel, R. M. Fleming, J. M. Phillips, and R. Ramesh, *Appl. Phys. Lett.* **64**, 3045 (1994).
²E. Favre-Nicolin and L. Ranno, *J. Magn. Magn. Mater.* **272–276**, 1814 (2004); J.-B. Yau, X. Hong, A. Posadas, C. H. Ahn, W. Gao, E. Altman, Y. Bason, L. Klein, M. Sidorov, and Z. Krivokapic, *J. Appl. Phys.* **102**, 103901 (2007).
³I. C. Infante, V. Laukhin, F. Sánchez, and J. Fontcuberta, *Mater. Sci. Eng., B* **126**, 283 (2006); X. Jin, R. Ramos, Y. Zhou, C. McEvoy, and I. V. Shvets, *J. Appl. Phys.* **99**, 08C509 (2006).

- ⁴Y. Bason, J. Hoffman, C. H. Ahn, and L. Klein, *Phys. Rev. B* **79**, 092406 (2009).
⁵R. P. van Gorkom, J. Caro, T. M. Klapwijk, and S. Radelaar, *Phys. Rev. B* **63**, 134432 (2001).
⁶R. Ramos, S. K. Arora, and I. V. Shvets, *Phys. Rev. B* **78**, 214402 (2008).
⁷X. Hong, A. Posadas, A. Lin, and C. H. Ahn, *Phys. Rev. B* **68**, 134415 (2003).
⁸M. C. Smoak, P. A. Ryan, F. Tsui, T. K. Nath, R. A. Rao, D. Lavric, and C. B. Eom, *J. Appl. Phys.* **87**, 6764 (2000).
⁹J. O'Donnell, M. Onellion, M. S. Rzchowski, J. N. Eckstein, and I. Bozovic, *J. Appl. Phys.* **81**, 4961 (1997).
¹⁰W. Limmer, J. Daeubler, L. Dreher, M. Glunk, W. Schoch, S. Schwaiger, and R. Sauer, *Phys. Rev. B* **77**, 205210 (2008).
¹¹A. Schuhl, F. Nguyen Van Dau, and J. R. Childress, *Appl. Phys. Lett.* **66**, 2751 (1995).
¹²Y. Bason, L. Klein, J.-B. Yau, X. Hong, J. Hoffman, and C. H. Ahn, *J. Appl. Phys.* **99**, 08R701 (2006).